In-phantom depth-dose measurements in mammography utilizing a Compton spectrometer

Tania A. C. Furquim [b*], Ricardo A. Terini [a], Silvio B. Herdade [b]

[a] Pontificia Universidade Católica de de São Paulo, Departamento de Física, R. Marquês de Paranaguá , 111, 01303-050, São Paulo, SP, Brasil.

[b] Universidade de São Paulo, Instituto de Eletrotécnica e Energia, Av.Prof. Luciano Gualberto, 1289, 05508-010, São Paulo, SP, Brasil.

Abstract. Mammography, using X-rays, is routinely utilized for screening of patients for prevention of breast cancer. Nevertheless, there is a small but significant risk of radiation induced carcinogenenesis associated with radiation exposure of the breast, being glandular tissue the most sensitive one among the tissues composing breast. Risk estimation in mammography may be determined by the mean absorbed dose in the glandular tissue, $<D_g>$. It is impossible to measure $<D_g>$ directly. Conversion factors are used to derive $<D_g>$ from measurements of incident exposure or kerma in free air, which may be obtained by Monte Carlo calculations in mathematical breast models, or from depth-dose measurements in homogeneous breast phantoms. In this work, X-ray beams from two apparatuses have been used in connection with a BR-12 mammography phantom: a GE Senographe 700T clinical unit, Mo anode/Mo filter, and a Philips constant potential equipment, W anode/Mo filter. $<D_g>$ values have been determined by two procedures: (a) by measurement of the incident air kerma, using an ionization chamber, multiplied by conversion factors from the literature, determined by Monte Carlo calculations on the basis of breast models; (b) by obtaining the incident air kerma and the dose, in several depths in a BR-12 phantom, by means of X-ray energy spectra measured with a Compton spectrometer. In this spectrometer, the radiation scattered by a small cylindrical Lucite probe, located over or inside the phantom, is detected, at an angle of about 90^o with the direction of the primary beam, by a CdTe semiconductor detector. The air kerma and in-phantom depth-doses, in the X-ray primary beam, are obtained by utilizing the Klein-Nishina cross-section and parameters of the experimental setup. Depth-dose curves and $<D_g>$ results normalized for unit incident air kerma were obtained for both systems and are presented for 30 kV.

KEYWORDS: Compton spectrometry, mammography, depth-dose, CdTe detector, BR-12 phantom.

1. Introduction

Mammography using an X-ray emitter is still considered the best method for screening of patients in the prevention of breast cancer. Nevertheless, in this procedure, there is a small but significant risk of radiation induced carcinogenesis associated with the exposure of the breast. Therefore, the concept of ALARA should also be applied for the radiation doses in mammography. Breast dosimetry has been reviewed by Dance et al. [1]. Glandular tissue is considered to be the most sensitive one among the tissues composing breast with respect to carcinogenesis [2]

Risk estimations in mammography may be determined by the mean absorbed dose in the glandular tissue $<D_g>$. It is impossible to measure $<D_g>$ directly. Therefore, conversion factors are used to derive $<D_g>$ from measurements of incident exposure or air kerma. Conversion factors may be obtained by Monte Carlo calculations in mathematical breast models [3-7], or from depth-dose measurements in homogeneous breast phantoms [8-9]. Depth-dose measurements have been carried out by utilizing TLD chips or an ionization chamber [10].

In this work, in-phantom depth dose distributions in mammography have been measured by means of a Compton spectrometer [11-13], utilizing plates of a BR-12 phantom material (50%-50% glandular-adipose tissues) in the X-ray beams of two apparatuses: a GE Senographe 700T clinical unit, Mo anode/Mo filter, and a Philips industrial constant potential equipment, with W anode/ Mo filter. In the utilized Compton-scatter method, a small probe, acting as a scatterer (a cylindrical Lucite rod 6 mm in diameter), located in the primary beam, was positioned substituting a plate in several depths in the phantom. The scattered photons were detected at a small distance from the Lucite probe by a CdTe

detector, at an angle of about 90^{o} with the direction of the primary beam. The validity of the Compton scatter method has been checked by comparison of HVL measurements using this technique with corresponding values obtained using a calibrated mammography ionization chamber. On-site $<D_g>$ estimations may be obtained, for a given HVL, by utilizing depth-dose data presented in this work. Mean glandular dose $<D_g>_N$ normalized to unit incident air kerma, from depth dose measurements presented in this paper, has been compared with the results obtained by a procedure routinely used for quality control in mammography [18].

2. Materials and Methods

2.1 Materials

2.1.1 X-ray apparatuses

(a) GE Senographe model 700T, focal spots of 0.3 mm and 0.1 mm, Mo anode/0.03 mm Mo filter, 0.69 mm beryllium window, and an additional collimator lead plate 1 mm thick, with 10 mm diameter hole, operated in the range 25 to 35 kV (b) Philips industrial constant potential generator, focal spots 1.2 mm and 4 mm, conical lead collimator, W anode/ 0.06 mm Mo filter. In both cases the larger focal spots have been used.

2.1.2 Compton spectrometer [11-13]

X-ray Compton scattering device: Lucite (PMMA) cylindrical rod with diameter of 6 mm.
Photon detecting system: Amptek Inc., consisting of a cadmium telluride detector (model XR-100T-CdTe), with area 3 x 3 mm^2, nominal thickness 1 mm, 250 μm beryllium window, cooled by thermoelectric (Peltier) cooler (at -30^{o} C), a power supply and amplifier module (model PX2T), a pocket multichannel analyser (model MCA 8000A), and a desk or laptop computer. A tungsten collimator, with 2 mm thickness and 2 mm hole diameter, together with a 3 mm diameter x 6 cm length cylinder, made of lead and internally with copper, has been used in front of the CdTe detector to reduce the angle of detection of the radiation to about 3^{o}. The energy calibration of the X-ray detecting system has been carried out using standard X- and gamma ray radioactive sources of ^{241}Am and ^{133}Ba. The full energy intrinsic efficiency of the system was determined experimentally by the ratio of the measured to the foreseen intensities of the sources spectral lines. A semi-empirical function was fitted to the data and used to correct all measured spectra. The X-rays measured spectra were previously corrected for Te and Cd K-escape peaks.

2.1.3 Mammography phantom

BR-12 mammography phantom (50% glandular - 50% adipose tissues) (Nuclear Associates, NY,USA), formed by rectangular plates with area 125 mm x 100 mm (3 plates 20 mm thick, 2 plates 10 mm thick, 1 plate 5 mm thick). With the combination of these plates it is possible to measure in-phantom doses in several depths.

2.1.4 Mammography ion chamber

Ionization chamber 10x5-6M, coupled to a radiation monitor model 9095, both manufactured by Radcal (Radcal Co., Monrovia, CA, USA), calibrated and presenting a constant energy response from 0.05 to 2.0 mm Al (HVL).

2.2 Methods

2.2.1 Experimental setup and procedure for measurement of the scattered beam spectra.

Figure 1 shows the experimental setup used for measuring photon spectra scattered by the 6 mm Lucite (PMMA) rod, positioned at an air gap inside the phantom, under a certain thickness of BR-12

material, in the primary beam of the GE Senographe 700T apparatus. A similar setup was used with the Philips constant potential equipment.
The scattered X-ray spectra have been corrected taking into account the full energy intrinsic efficiency of the detector and attenuation of photons by the materials located between the Lucite scatterer and the sensitive region of the detector. The Compton scattered photon energies are given by:

$$E' = E.\left[\frac{1}{1+\alpha.(1-\cos\theta)}\right] \quad (1)$$

where E is the energy of the incident photon, Θ is the scattering angle and

$$\alpha = E/\, m_0\, c^2 = E\ (\text{keV}) / 511\ \text{keV} \quad (2)$$

being m_0 = electron rest mass , c = speed of light in vacuum. After determining *E'* from the shift of the scattered X-ray spectra, the scattering angle Θ has been determined in this work by the expression derived from equation (1):

$$\theta = \cos^{-1}\left[1-511.\left(\frac{E-E'}{E.E'}\right)\right] \quad (3)$$

Figure 1: Experimental setup showing the CdTe spectrometer (1), PMMA scatterer (2) between BR12 phantom slabs (3), which is in turn between the compression paddle (4) and the image receptor (5) at the mammography equipment.

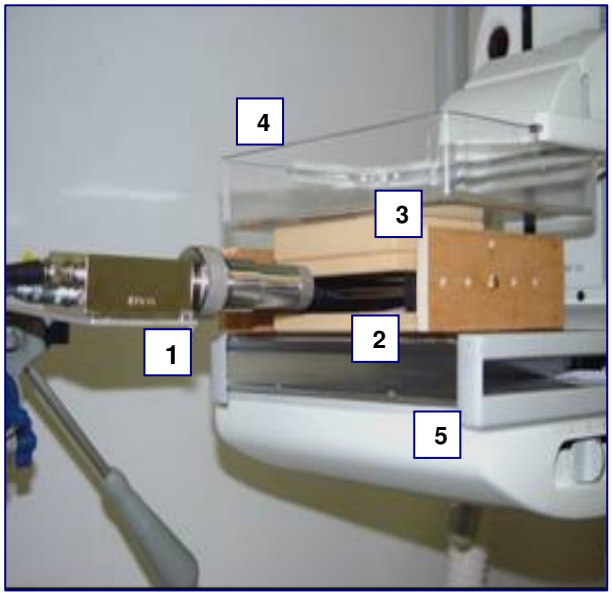

2.2.2 Reconstruction of the primary beam spectra from the scattered beam spectra.

Compton scattering is an incoherent inelastic process. To reconstruct the primary beam spectra from the scattered beam spectra using the Compton effect, the elastic coherent scattering contribution, that is important in the mammography energy range, must be subtracted [13-14]. In the reconstruction procedure, a method proposed by Yaffe et al. [11] and Matscheko et al. [12] has been applied. The incident primary fluence rate, $d\Phi/d\Theta(E,\Theta)$, is obtained from the Compton scattered rate of photons incident on the detector, $N_{d,inc}(E',\Theta)$, by means of the Klein-Nishina cross-section, $d\sigma/d\Omega(E,\Theta)$ (corrected for the binding energy of the atoms in the scatterer), using published values of molecular form factors and incoherent scattering functions [15,16] as well as parameters of the

experimental setup. Primary beam fluence may be converted into exposure (C/Kg), kerma or dose (Gy), by applying the corresponding conversion factor.

2.2.3 Determination of $<D_g>$ from in-phantom depth dose measurements.

Hammerstein et al. [9] proposed a simple model (see Figure 1.c in reference [8]) for computing $<D_g>$ in a firmly compressed breast, making several assumptions: (a) dose to the skin and areola can be ignored; (b) adipose tissue 0.5 cm thick encloses a central glandular region consisting of a mixture of adipose and glandular tissue; and (c) compression produces a volume of rectangular cross section. Using this model, mean glandular dose per view, normalized to unit incident air kerma, $<D_g>_N$, is given by [8]:

$$< D_g >_N = f_g . B . < \chi >_g \quad (4)$$

where:

f_g is the absorbed dose – to – air kerma conversion factor (glandular tissue); B is the backscatter factor of the BR-12 phantom at a certain HVL; and

$$< \chi >_g = \frac{1}{\tau - 1} . \int_{0.5}^{\tau - 0.5} \chi_g (z) dz \quad (5)$$

being τ = phantom thickness; and $\chi_g(z) = K_g(z)/K_S$, with $K_g(z)$ = air kerma at depth z of the glandular tissue, K_S = air kerma at surface.

Mean glandular dose, $<D_g>$, is a function of half-value layer (HVL), X-ray tube target material and angle, X-ray tube potential, phantom thickness and composition.
In the showed measurements, $K_g(z)$ stands for the air kerma value measured in the air gap located between the phantom slabs, at a depth z from the entrance surface.

2.2.4 Determination of $<D_g>$ from the measurement of the entrance air kerma in a BR-12 phantom.

The mean glandular dose, $<D_g>$, may be estimated from the measurement of the entrance air kerma in a BR-12 phantom. In this paper, two kinds of measurements were used: with backscatter, utilizing conversion factor of Wu et al. [3-5]**;** and without backscatter, with compression, using conversion factors of Dance *et al*. [6-7] for 40-49 years old patients According to Wu *et al* [3], $<D_g>$ was determined by the relation $<D_g> = <D_g>_N$ **.** ESAK, where $<D_g>_N$ is the normalized mean glandular dose (mean glandular dose per unit entrance skin air kerma) and ESAK is the entrance skin air kerma. $<D_g>_N$ is assumed to be a function of the beam quality (HVL), X-ray tube target material, X-ray tube potential, breast thickness and breast composition. According to Dance *et al*., $<D_g>$ was estimated by

$$< D_g > = K_S . p . g \quad (6)$$

where K_S is the incident air kerma, p converts K_S to the phantom to that for the standard breast, and g converts K_S to $< D_g >$ [17].

3. Results

The obtained primary beam spectra at several depths in the phantom have been converted into air kerma and absorbed dose by utilizing photon data from the literature. Dose versus depth distributions in phantom have been determined by the spectroscopic method described above for the two mentioned apparatus, in the range of voltages from 25 to 35 kV. In this paper, we present results for 30 kV (see Figs. 2 and 3).

As the geometry of spectrometric detection is not trivial (the scatterer acts as a cylindrical photon source perpendicular to the detector axis), the solid angle of detection Ω was determined here normalizing the spectral results to those obtained with the calibrated ionization chamber. Thus, we compared obtained $<D_g>_N$ values (see Tables 1 and 2). For the W/Mo combination, it is to be noted that the HVL determined without the compression paddle was 0.37 mmAl, from the measurements with ionization chamber, and 0.36 mmAl, from the spectral measurements, in good agreement with the results reported by Kessler [18], 0.364 mmAl, using a clinical equipment.

Table 1: Values of incident beam HVL, ESAK, $<D_g>_N$ and $<D_g>$ obtained with the mammography Mo/Mo equipment, with compression paddle, from the ionization chamber and Compton spectrometer measurements, for 30 kV and 100 mAs, with total BR-12 thickness of 6 cm.

Ionization chamber					**Compton spectrometer**			**Determined Ω** (sr)
HVL (mm Al)	**ESAK** (mGy)	**$<D_g>_N$**	**$<D_g>$ (Wu)** (mGy)	**$<D_g>$ (Dance)** (mGy)	**HVL** (mm Al)	**ESAK** (mGy)	**$<D_g>_N$**	
0.408	12.89	0.163	2.121	2.753	0.400	12.89	0.072	$1.51 \cdot 10^{-4}$

Figure 2: Comparison between 30 kV determined primary beam air kerma spectra, without phantom and at a depth of 2 cm of BR-12 phantom, for Mo/Mo combination.

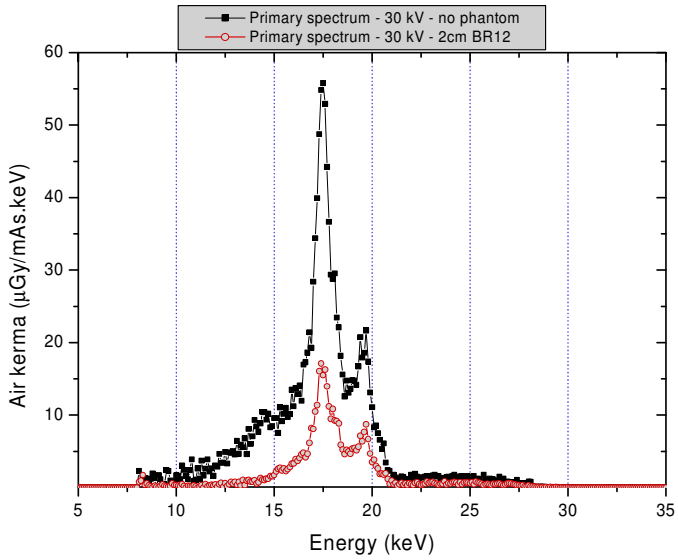

Table 2: Values of incident beam HVL, ESAK rate, $<D_g>_N$ and $<D_g>$ obtained with the industrial W/Mo equipment, with the same compression paddle, from the ionization chamber and Compton spectrometer measurements, for 30 kV and 25 mA, 4s (100mAs), with total BR-12 thickness 6 cm.

Ionization chamber				**Compton spectrometer**			**Determined Ω** (sr)
HVL (mm Al)	**ESAK** rate (mGy/min)	**$<D_g>_N$**	**$<D_g>$ (Wu)** (mGy)	**HVL** (mm Al)	**ESAK** rate (mGy /min)	**$<D_g>_N$**	
0.411	51.828	0.182	3.456	0.414	51.828	0.148	$6{,}69 \cdot 10^{-5}$

Figure 3: Comparison between 30 kV determined primary beam air kerma spectra, normalized by maxima, incident on phantom surface and at a depth of 4 cm of BR-12, for the W / Mo equipment.

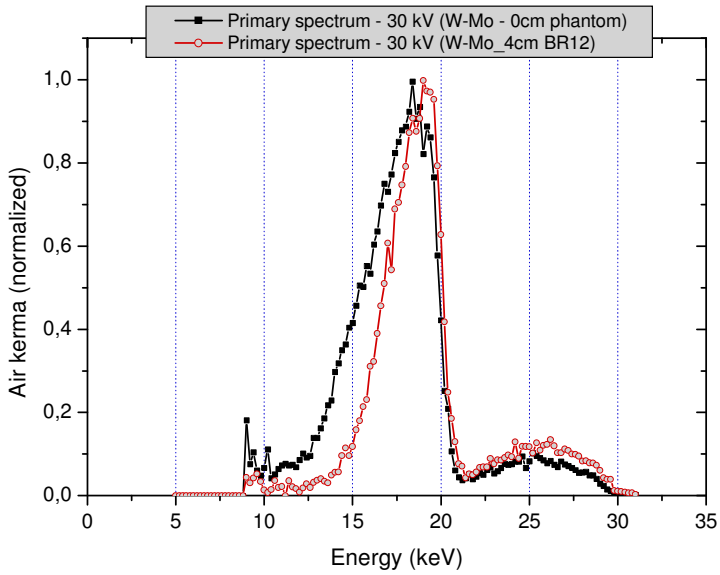

Figure 4: Depth-dose curves obtained for BR-12, with 6cm total thickness, in both situations: Mo/Mo (mammography unit) (*blue line*) and W/Mo (*red line*) combinations.

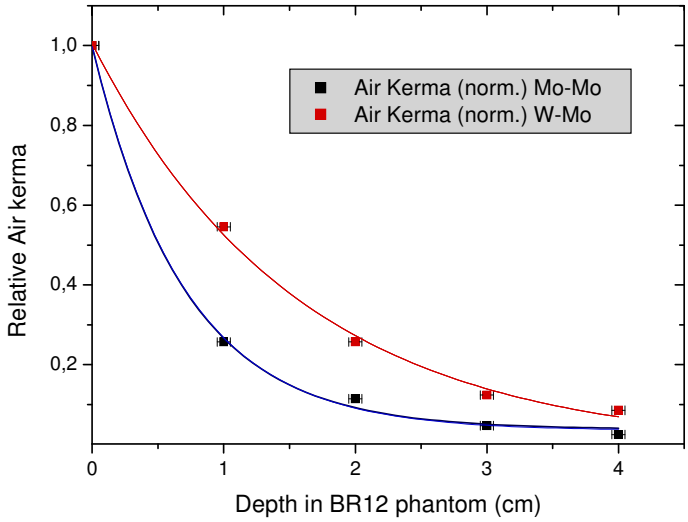

4. Discussion

In this paper, we have shown results about depth-dose distributions and X-ray spectra in mammography for Mo/Mo and W/60µmMo anode/filter combinations, with BR-12 phantom slabs, as well as values of normalized mean glandular dose from spectral and dosimetric measurements.
The primary spectra have been obtained from Compton scattering spectrometry measurements.
The behaviour of depth-dose curve for BR-12 material, with Mo/Mo combination was similar to, but systematically lower than that obtained by Stanton *et al.*[8]. Differences could be attributed mainly to the air gap introduced in the phantom by the presence of the scatterer and its holder.
We didn't find any results concerning depth-dose for W/Mo combinations.

The method ensures determination of absorbed doses in a breast equivalent phantom together with the respective incident beam spectrum.
In the near future, we intend to improve the setup to study the influence of displacement and air gap in the obtained results, like in ref. [19].

Figure 5: Depth-dose curves obtained for BR-12, with 6cm total thickness, for Mo/Mo (mammography unit) (*blue line*) together with similar results obtained by Stanton *et al*.[8] (*red line*).

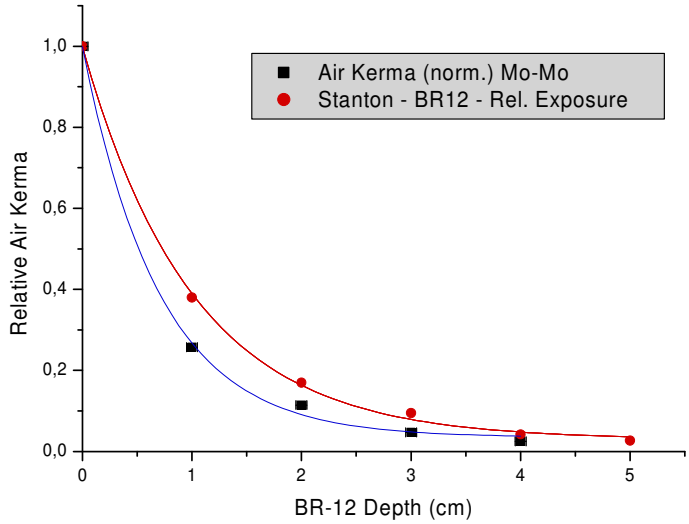

Acknowledgements

We would want to thank IAEA by the providing of the mammography equipment, Brazilian agencies FAPESP and CNPq by the financial support and IEE-USP by the use of infra-structure and staff help. We also would like to thank the help of the undergraduate student Jose Neres de Almeida Jr. (PUC-SP).

REFERENCES

[1] DANCE D.R. et al., "Breast dosimetry", Appl. Rad. Isot. 50 (1999) 185-203.
[2] NATIONAL COUNCIL ON RADIATION PROTECTION, Mammography: A User' Guide. Report 85, (Bethesda, MD: NCRP Publications)(1986).
[3] WU X. et al., "Spectral dependence of tissue glandular dose in screen-film mammography", Radiology 179 (1991) 143-148..
[4] WU X. et al., "Normalised average glandular dose in molybdenum target-rhodium filter and rhodium target –rhodium filter mammography", Radiology 193 (1994) 83-89..
[5] SOBOL W.T. et al., "Parametrization of mammography normalized average glandular dose tables", Medical Physics 24 (1997) 547-5
[6] DANCE D.R. et al., "Monte Carlo calculation of conversion factors for the estimation of mean glandular breast dose", Phys. Med. Biol. 35 (1990) 1211-1219.
[7] DANCE D.R. et al., "Additional factors for the estimation of mean glandular breast dose using the UK mammography dosimetry protocol ", Phys. Med. Biol. 45 (2000) 3225-3240.
[8] STANTON L. et al., "Dosage Evaluation in Mammography ", Radiology 150 (1984) 577-584.
[9] HAMMERSTEIN G.R. et al., "Absorbed radiation dose in mammography", Radiology 130 (1979), 485-491.

[10] STANTON L. et al., “Comparison of ion chamber and TLD dosimetry in mammography”, Med. Phys. 8 (1981) 792-798.
[11] YAFFE M. et al., “Spectroscopy of diagnostic X-rays by a Compton-scatter method”, Med. Phys. 3 (1976) 328-334.
[12] MATSCHEKO G. et al., “A Compton scattering spectrometer for determining X-ray photon spectra”, Phys. Med. Biol. 32 (1987) 577-594.
[13] VIEIRA A. A. et al., “Compton Spectrometer for X-rays in the Energy Range from 10 to 150 keV”, Proceedings of the INTERNATIONAL NUCLEAR ATLANTIC CONFERENCE - INAC 2007, Santos, SP, Brazil, September 30 to October 5, 2007.
[14] JOHNS H.E. et al, “The physics if radiology”, 4th ed. (Charles C. Thomas, Springfield, USA), 1986.
[15] TARTARI A, CASNATI E, BONIFAZZI C, BARALDI C., “Molecular differential cross section for x-ray coherent scattering in fat and polymethyl methacrylate”, Phys. Med. Biol. 42 (1997), 2551-2560.
[16] HUBBELL J H, VEIGELE W J, BRIGGS E A, BROWN R T, CROMER D T, HOWERTON R J., “Atomic form factors, incoherent scattering functions and photons scattering cross sections”, J. Phys. Chem. Ref. Data 4 (1975), 471-538.
[17] FURQUIM T.A.C., “Metodología para correlação entre doses e detectabilidade em imagens mamográficas padrões: aplicação no Estado de São Paulo”, PhD Thesis, Instituto de Pesquisas Energéticas e Nucleares (IPEN), Comissão Nacional de Energia Nuclear (CNEN), SP (2005).
[18] KESSLER C., “Mamographic dosimetry”, CCRI(I)/05-26, BIPM, Sèvres.
[19] ZOETELIEF, J., WIT, N.J.P., BROERSE, J.J., “Dosimetric Aspects of film/screen mammography: In-phantom dosimetry with thimble-type ionisation chambers”, Phys. Med. Biol. 34 (1989) 1169-1177.